

# RSC Advances



This is an *Accepted Manuscript*, which has been through the Royal Society of Chemistry peer review process and has been accepted for publication.

*Accepted Manuscripts* are published online shortly after acceptance, before technical editing, formatting and proof reading. Using this free service, authors can make their results available to the community, in citable form, before we publish the edited article. This *Accepted Manuscript* will be replaced by the edited, formatted and paginated article as soon as this is available.

You can find more information about *Accepted Manuscripts* in the [Information for Authors](#).

Please note that technical editing may introduce minor changes to the text and/or graphics, which may alter content. The journal's standard [Terms & Conditions](#) and the [Ethical guidelines](#) still apply. In no event shall the Royal Society of Chemistry be held responsible for any errors or omissions in this *Accepted Manuscript* or any consequences arising from the use of any information it contains.

## ARTICLE

# Hyaluronic acid-PEI-Cyclodextrin polyplexes: Implications on *in vitro* and *in vivo* transfection efficiency and toxicity

Cite this: DOI: 10.1039/x0xx00000x

S. Jain<sup>a\*</sup>, S. Kumar<sup>a, b</sup>, A. K. Agrawal<sup>a</sup>, K. Thanki<sup>a</sup>, U. C. Banerjee<sup>b</sup>

Received 00th January 2012,

Accepted 00th January 2012

DOI: 10.1039/x0xx00000x

www.rsc.org/

The present study reveals novel HA-PEI-CyD polyplexes as, non-viral vector, for gene delivery. The conjugate was synthesized and phenol-sulfuric acid method revealed ~5 and 60% grafting of cyclodextrin and hyaluronic acid, respectively, in the final conjugate. Model plasmid DNA, pEGFP-N3, was complexed with synthesized HA-PEI-CyD and N/P ratio 10 was found optimum and exhibited excellent stability in presence of serum and DNase I. *In vitro* transfection of HA-PEI-CyD polyplexes in HeLa, HEK-293 and MCF-7 cells revealed ~39.5, 41.4 and 8.8 fold higher transfection as compared to plain PEI, respectively. Confocal laser scanning microscopy confirmed the higher cellular uptake and efficient nuclear colocalization of the HA-PEI-CyD polyplexes. MTT assay revealed >90% cell viability in HA-PEI-CyD polyplexes in contrast to ~20% cell viability in plain PEI. Furthermore, excellent GFP expression in tumor bearing animals and significantly lower *in vivo* toxicity along with hemocompatibility demonstrated the suitability of proposed conjugate for gene delivery.

## 1. Introduction

Gene therapy has been evolved as a potential therapeutic strategy for various stubborn human diseases since last few decades. Therapeutic effectiveness and safety of gene therapy not only depends on gene construct but also on the ability of ferrying cargo to deliver the gene construct to its target site while avoiding deleterious consequences to normal cells. Immunogenicity and associated risk with the conventional viral vectors resulted in emergence of better non-viral vectors as a potential alternative to them.<sup>1,2</sup> Advantages, like ease of preparation, non-immunogenicity, ability to shield the DNA against nucleases, high DNA loading capacity, feasibility of attaching targeting ligand and low cost associated with non-viral vectors 3-5 shifted the focus of scientific community towards this germane area which introduced a number of non-viral vectors viz. cationic polymers, cationic liposomes and dendrimers for gene delivery.<sup>1,2,6,7</sup> These cationic vehicles electrostatically interact with negatively charged phosphate groups of DNA and condense DNA to submicron size particles facilitating its cellular uptake.<sup>8</sup>

Among the cationic polymers, polyethylenimine (PEI) has been recognized as a potential delivery reagent, primarily due to its excellent transfection efficiency assisted by proton sponge effect and protection of DNA degradation against harsh lysosomal environment.<sup>9</sup> However, excessive cationic charge density on PEI results into interference with protein kinase C leading to apoptosis and cytotoxicity and tendency to form larger aggregates with negatively charged blood components. This pushes it at back row among the novel non-viral transfection reagents.<sup>10,11</sup>

Over time PEGylation and coating of polysaccharides came into picture to modify the polycationic surface of PEI.<sup>12,13</sup> Although PEGylated PEI exhibited reduced toxicity yet, no improvement was observed in transfection efficiency.<sup>14</sup> In another approach, polysaccharide coating was found superior as it imparted physicochemical stability along with site specificity which resulted

in improved transfection efficiency with reduced cytotoxicity.<sup>15,16</sup>

This concept was also observed and supported by our previous work in which hyaluronic acid-PEI (HA-PEI) and chondroitin sulfate-PEI (CS-PEI) were found to have higher transfection efficiency and reduced cytotoxicity in comparison with parent PEI.<sup>17,18</sup>

Cyclodextrins (CyD) containing polycations has been explored as non-viral nanocarriers for gene therapy and exhibits higher transfection vis-à-vis lesser toxicity in comparison with non CyD containing polycations.<sup>19,20</sup> Therefore, we hypothesized that inclusion of CyD into HA-PEI and CS-PEI may further fortify the performance of these complexes. This presumption was based on the dual specification provided viz. formation of inclusion complex by guest host interaction, stability and target specificity due to CyD and HA, respectively. Thus in the present study, HA-PEI-CyD based polyplexes were developed and evaluated for transfection efficiency, cellular uptake and nuclear colocalization and cytotoxicity in different cell lines. Finally *in vivo* gene expression, toxicity in appropriate animal models and hemocompatibility were also checked.

## 2. Materials and Methods

### 2.1 Materials

Branched PEI (MW 25 kDa),  $\beta$ -Cyclodextrin (CyD), carbonyldiimidazole (CDI), 3-(4,5-dimethylthiazol-2-yl)-2,5-diphenyltetrazolium bromide (MTT), anhydrous DMF, Tris, bromophenol blue (BPB), ethidium bromide (EtBr) and xylene cyanol (XC), 4',6-diamidino-2-phenylindole dihydrochloride (DAPI), rhodamine isothiocyanate (RITC), DMBA (7,12-Dimethylbenz anthracene) were procured from Sigma-Aldrich Chemical Co., St. Louis, MO, USA. Dialysis membrane (MWCO 25 kDa) was procured from Spectrum Labs USA. Hyaluronic acid (MW 5 kDa) was provided as generous gift sample from Focaschem Biotech limited, China. Plasmid (pEGFP-N3, 4.7 kb) encoded for enhanced green fluorescence protein was

procured from Addgene. MCF-7 (Human breast adenocarcinoma), HeLa (Human cervix adenocarcinoma) and HEK-293 (Human embryonic kidney-293) cell lines were obtained from the cell repository facility of National Centre for Cell Sciences (NCCS), Pune, India. DNase was purchased from Fermentas Molecular Biology Tools. Deionized (MilliQ) and Millipore filtered (pore diameter 0.22  $\mu\text{m}$ ) water was used throughout the experiments. All other chemicals and reagents were of analytical grade and procured from local suppliers.

## 2.2 Synthesis and characterization of HA-PEI-CyD

The synthesis of HA-PEI-CyD was carried out in two steps. In step 1 CyD-PEI backbone was synthesized by previously reported method. Briefly, the hydroxyl groups of CyD were activated by dissolving CyD (0.015 mmol, 100 mg) in 20 mL anhydrous N,N-dimethylformamide (DMF) followed by drop wise addition of CDI (0.10 mmol). The mixture was stirred at room temperature for 1 h and then precipitated in cold diethylether and washed three times with diethylether to remove unreacted material. The resulting CyD-CDI was filtered; residue was dissolved in 10 mL DMF and stored at 4°C until use. PEI (0.010 mmol, 250 mg) was dissolved in DMF containing 100  $\mu\text{L}$  of triethylamine (Et<sub>3</sub>N) followed by drop wise addition of CyD-CDI solution over 2 h with continuous stirring. The stirring was continued for additional 4 h to allow the reaction to complete. The mixture was then dialyzed overnight using dialysis tubing (MWCO, 25 kDa) in water and freeze-dried. In next step, solutions of different concentration of HA (5, 10 and 15% w/v) in water were added to the aqueous solution of PEI-CyD solution followed by continuous stirring up to 24 h and dialysis for next 24 h, which resulted in formation of HA-PEI-CyD1, HA-PEI-CyD2 and HA-PEI-CyD3, respectively.

The concentration of CyD and HA in PEI-CyD and HA-PEI-CyD was determined using phenol-sulphuric acid method.<sup>21</sup> Briefly, 25  $\mu\text{L}$  of PEI-CyD/HA-PEI-CyD (1  $\mu\text{g}/\mu\text{L}$ ) was mixed thoroughly with 15  $\mu\text{L}$  fresh 5% (w/v) phenol solution in double distilled water and 90  $\mu\text{L}$  concentrated H<sub>2</sub>SO<sub>4</sub> (95–97%) followed by incubation for 30 min at room temperature. Following incubation, samples were diluted up to 1 mL and the absorbance was recorded at 490 nm on UV-VIS spectrophotometer (Shimadzu, UV-1800). Proton NMR was used to further characterize the synthesized complex. For analysis, 2 mg of complex was dissolved in 0.5 mL of D<sub>2</sub>O and <sup>1</sup>H spectrum of each sample was recorded with a NMR spectrometer (400 MHz; Bruker Corporation). The synthesis of PEI-CyD and HA-PEI-CyD was confirmed by proton NMR.

## 2.3 Preparation and evaluation of HA-PEI-CyD/pDNA polyplexes

Polyplexes were formed at different N/P ratios (1.25, 2.5, 5, 7.5 and 10) by simply mixing the varying concentration of HA-PEI-CyD with pDNA solution in equivalent volume followed by vortexing for 15 sec and incubation at room temperature for 20 min. All the polyplexes had the final pDNA concentration of 2  $\mu\text{g}/\text{mL}$ . Here N/P ratio represents ratio of moles of the positively charged amino groups of cationic polymers to the mole of negatively charged phosphate groups of DNA. Polyplexes were characterized for size, polydispersity index (PDI) and zeta potential by using zetasizer (Nano ZS, Malvern, UK). Shape and morphology of the optimized complex was studied by using scanning electron microscopy (SEM, Hitachi, S-3400N, Japan) after gold coating and atomic force microscopy (AFM, Veeco, di Bioscope SZ).<sup>22-24</sup>

## 2.4 Optimization of N/P ratio: Agarose gel electrophoresis

For gel electrophoresis, polyplexes were gently mixed with loading buffer containing xylene cyanol, a tracking dye, and loaded into individual wells of 0.8% agarose gel and electrophoresed at 100 V for 45 min in TAE buffer (40 mM Tris-HCl, 1% (v/v) acetic acid, 1 mM EDTA). The gels were stained using ethidium bromide (EtBr) and the bands corresponding to pDNA were visualized under a UV transilluminator.<sup>17, 18</sup>

## 2.5 DNase protection assay

The ability of developed polyplexes to protect the complexed DNA against DNase-I was evaluated by DNase protection assay.<sup>25</sup> Briefly, naked plasmid DNA and different polyplexes (formed at N/P ratio 10) were incubated at 37°C for 30 min in buffer solution (10 $\times$ 10<sup>-3</sup> M Tris-Cl, 150 $\times$ 10<sup>-3</sup> M NaCl, 1 $\times$ 10<sup>-3</sup> M MgCl<sub>2</sub>, pH 7.4) containing 10  $\mu\text{L}$  DNase I (1000 units/mL). Additionally, 50  $\mu\text{L}$  of Mg<sup>2+</sup> solution (50 $\times$ 10<sup>-3</sup> M) was also added to initiate the enzymatic reaction. The change in absorbance value was measured spectrophotometrically at 260 nm at the interval of 2 min.

In another method, protection against DNase I was confirmed by gel electrophoresis. The procedure was same as described above followed by inactivation of DNase I with the addition of 5  $\mu\text{L}$  100 mM EDTA (10 min). Subsequently, the complexes were incubated in presence of 10  $\mu\text{L}$  heparin (5 mg/mL) for 2 h to dissociate the complexes. The samples were electrophoresed in 0.8% agarose to examine pDNA released from the complex.

## 2.6 Serum stability

In vitro serum stability of the developed polyplexes was determined by measuring changes in the critical quality attributes (particle size and zeta potential) and by EtBr intercalation assay.<sup>26</sup> Briefly, naked plasmid DNA and different polyplexes (at N/P ratio 10) were incubated at 37°C for different time points (0.5, 1, 2 and 4 h) with equal volume of PBS buffer (pH 7.4) containing 20% FBS to have 10% of FBS in the final mixture. Following incubation, samples (1 mL) at corresponding time points were mixed with EtBr solution in water to get the final concentration, 0.2  $\mu\text{g}/\text{mL}$  of EtBr. Fluorescent intensity of the resultant mixtures was determined at 516 nm, excitation wavelength and 618 nm, emission wavelength. The % change in EtBr fluorescence was calculated as a fraction of observed fluorescence to maximum fluorescence, obtained upon addition of EtBr to free plasmid. The sample collected after 4 h of incubation were also examined for change in particle size and zeta potential before processing for EtBr intercalation assay.

## 2.7 In vitro transfection, cytotoxicity, cellular uptake and colocalization studies

### 2.7.1 In vitro transfection

Cells were maintained by following our previous reported protocol.<sup>22</sup> HeLa, HEK-293 and MCF-7 cells (1 $\times$ 10<sup>5</sup> cells/well) were incubated at 37°C in six well plates with different polyplexes (N/P ratio 10) for 4 h in MEM having 10% FBS in the final mixture. Following which, cells were washed three times with PBS (pH7.4) and re-incubated at 37°C in fresh MEM having 10% FBS in the final mixture till 48 h. After incubation, cells were again washed thrice with PBS (pH7.4) and observed under confocal laser scanning microscopy (CLSM) (Olympus FV1000, Japan) using He-Ne green laser at 489 and 510 nm emission and excitation wavelength, respectively. Images were captured at 10x magnification. In separate set of experiments, the control and transfected cells were trypsinized and subjected to flow cytometry analysis using Guava easyCyte 8HT Benchtop Flow Cytometer (Millipore, USA) following standard protocol. Briefly, the samples were acquired using guavaSoft

Software and obtained plots—a Forward Scatter (FSC) vs Green Fluorescence (GRN-HLog) and dot plots were converted into histograms by plotting counts as a function of GRN-HLog. Two marker set were then applied for non-transfected (black colour) and transfected cells (green colour). All other parameters of the software were kept constant throughout the studies to normalize any possible variability. Further, protein expression level was also quantified using Bradford method while EGFP content in per mg of protein was determined by measuring fluorescent intensity. Briefly, incubated cells were washed with 50  $\mu$ L PBS and re-incubated with 100  $\mu$ L lysis buffer (10 mM Tris HCl, pH 7.4, 0.5% SDS, 0.5% Triton X-100, 1 mM EDTA). Cellular debris was pelleted by centrifugation at 10,000 rpm for 10 min. A 2  $\mu$ L of the supernatant was loaded on a Nanodrop spectrofluorimeter (NanoDrop 3300, Thermo Fisher Scientific, USA) and EGFP expression was estimated fluorimetrically at excitation and emission wavelength at 489 and 510 nm, respectively. EGFP expression of polyplexes was also measured against the blank cells (without pDNA).<sup>17,18</sup>

### 2.7.2 Cytotoxicity assay

Cytotoxicity of developed polyplexes was evaluated by standard MTT assay.<sup>17</sup> Briefly, cells attached to 96 well plates were incubated at 37°C with 100  $\mu$ L of developed polyplexes dispersions for 4 h, following which cells were washed thrice with PBS (pH 7.4) and re-incubated in fresh MEM containing 10% FBS till 48 h. Subsequently, medium was aspirated and 100  $\mu$ L of MTT (0.5 mg/mL in PBS) was added to each well. After 3 h, the supernatant was aspirated and 200  $\mu$ L of DMSO was added to each well. Formazan crystals were dissolved by gentle shaking of plates for one minute and absorbance was measured at 550 nm using ELISA plate reader (Biotek Inc., USA). All the experiments were performed in quadruplet. Untreated cells were taken as control with 100% viability and relative cell viability (%) was calculated using following formula:

$$\% \text{ Relative cell viability} = 100 \times \text{Abs (sample)} / \text{Abs (control)}$$

### 2.7.3 Cell uptake and nuclear colocalization studies

Cellular uptake and nuclear colocalization studies of different complexes were performed using CLSM. For the purpose RITC incorporated polyplexes were formed by first synthesizing RITC-PEI conjugate and subsequently using this conjugate in the formation of PEI, PEI-CyD and HA-PEI-CyD polyplexes. RITC-PEI was synthesized by dissolving RITC (0.5 mg/mL) in water simultaneously adjusting the pH to 8 and continuous stirring for 10 min. PEI (10 mg/mL) was added to RITC solution and reaction mixture was stirred in dark for 6 h to finally yield RITC-PEI. Similarly, RITC conjugated PEI-CyD and HA-PEI-CyD were synthesized.

Following overnight incubation, different cells, MCF-7, HeLa and HEK-293 were allowed to incubate with RITC incorporated polyplexes for 4 h. Following 4 h of incubation cells were thoroughly washed with PBS to remove the non-internalized complexes and fixed by adding 4% Paraformaldehyde in PBS (pH 7.4) for 10 minutes. After fixing cells were thoroughly washed with PBS and subjected to Triton X-100 (0.2% in PBS) for 2 min for permeabilization. Cells nuclei were counterstained with DAPI (1  $\mu$ g/mL in PBS) for 1 min followed by thorough washing with PBS.<sup>27</sup> The cells were visualized in CLSM (Olympus FV1000, Japan) at excitation/emission maxima ~358/461 for DAPI and ~560/580 maxima for RITC, respectively. Scatter plot analysis was performed for nuclear colocalization studies.

### 2.8 In vitro hemocompatibility

Blood was collected from rats in heparinized microcentrifuge tubes and subjected to centrifugation at 3000 rcf for 5 min at 4 °C to separate red blood cells (RBCs). The supernatant along with buffy clot was discarded and RBCs were washed thrice with isotonic PBS, pH 7.4. The stock of RBCs was prepared by mixing three volumes of RBCs with 11 parts of the PBS. A 100  $\mu$ L of this stock was mixed with PEI, PEI-CyD and PEI-CyD-HA complexes equivalent to 10  $\mu$ g/mL of PEI. RBCs, mixed with distilled water and PBS, were employed as positive and negative control, respectively. The samples were incubated at 37 °C for 3 h in a shaker bath and then centrifuged at 3000 rcf for 5 min to separate supernatant, which was allowed to stand at room temperature for 30 min to oxidize hemoglobin (Hb). The absorbance of oxygenated hemoglobin (Oxy-Hb) was measured spectrophotometrically at 540 nm, and percentage hemolysis was calculated by using following equation:

$$\% \text{ hemolysis} = \frac{AB_s}{AB_{100}} \times 100$$

where AB<sub>s</sub> is the absorbance of the sample and AB<sub>100</sub> is the absorbance of the control.

### 2.9 In vivo studies

#### 2.9.1 Animals

Animals were procured from central animal facility, NIPER and the protocols were duly approved by the Institutional Animal Ethics Committee (IAEC), NIPER, India. All the animal studies were performed in accordance with guidelines of the Committee for the Purpose of Control and Supervision of Experiments on Animals (CPCSEA), India. Animals were housed at temperature of 25±2°C and relative humidity of 50-60% under a 12 h light/dark cycles.

#### 2.9.2 In vivo gene expression

Female Sprague Dawley rats (200-250 g) were used for in vivo gene expression study. Cancer was induced following our previously reported protocol by oral administration of DMBA dissolved in soya bean oil at 45 mg/kg dose at weekly interval for three consecutive weeks.<sup>23</sup> After 10 weeks of the last dose of DMBA, tumor bearing animals were separated and naked DNA, and different complexes viz. PEI, PEI-CyD and PEI-CyD-HA (N/P ratio 10) were injected intratumorally. After 48 h of administration animals were humanely sacrificed and tumors were dissected and visualized under photon imager (Biospace, France) for fluorescence as a consequence of gene expression. The photon emission was measured dynamically (list-mode acquisition) using the large field-of-view setting and registered using the photon counting technology. During image analysis autofluorescence of the control animal (animals treated with naked DNA) was neutralized by increasing the threshold value.

#### 2.9.3 In vivo toxicity

Female Swiss Albino mice (25-30 g) were randomly divided into four groups (n=6) and treated with single administration of 100  $\mu$ L of individual complexes viz. PEI, PEI-CyD and PEI-CyD-HA. Group which didn't receive any formulation was taken as control. Blood samples were collected at day zero before initiating the study and after 15 days and analyzed for hematological parameters i.e., hemoglobin (Hb), RBC count, total leukocytes count and differential leukocytes counts. Additionally the levels of different biochemical markers viz. alanine transaminase (ALT), aspartate transaminase (AST), blood urea nitrogen (BUN) and creatinine were also examined using commercially available kits (Accurex, Biomedical Pvt. Ltd). In a separate set of study hemocompatibility was also evaluated by incubating different complexes with RBCs.<sup>28</sup>

## 2.10 Statistical Analysis

All results have been demonstrated as mean±standard deviation (SD). Statistical analysis was performed using Graph Pad Prism 6 using one-way analysis of variance (ANOVA) followed by Tukey-Kramer multiple comparison test.  $p < 0.05$  was considered as statistically significant.

## 3. Results

### 3.1 Synthesis and characterization of HA-PEI-CyD

The synthesis of PEI-CyD and HA-PEI-CyD was confirmed by proton NMR (Figure 1).

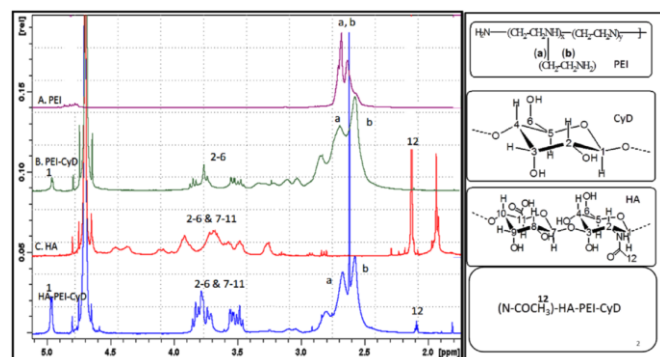


**Figure 1:** <sup>1</sup>HNMR of PEI, PEI-CyD, HA and HA-PEI-CyD

The signals from PEI ethylene protons (–CH<sub>2</sub>CH<sub>2</sub>NH–) appeared at  $\delta$  2.5–3.0 ppm while the C1 proton and C2–C6 protons of  $\beta$ -CyD appeared at  $\delta$  5 ppm and  $\delta$  3.0–4.0 ppm, respectively. The formation of HA-PEI-CyD was confirmed by the presence of apparent N-acetylate protons (–NCOCH<sub>3</sub>–) of HA at  $\delta$  2.1 ppm. The other proton peaks that ranged between  $\delta$  3.5–4.0 ppm could not be distinguished because of the overlap of glucose unit peak of HA and CyD. The % w/w grafting of CyD in PEI-CyD and HA in corresponding HA-PEI-CyD is shown in Table I.

**Table I:** % w/w grafting of CyD in PEI-CyD and HA in HA-PEI-CyD

	CyD grafting	HA grafting
PEI	-	-
PEI-CyD	4.8	-
HA-PEI-CyD1	4.8	4.3
HA-PEI-CyD2	4.8	9.4
HA-PEI-CyD3	4.8	14.2

Phenol-sulfuric acid method revealed 5 % and 60 % w/w grafting of CyD and HA in final complexes.

### 3.2 Preparation and evaluation of HA-PEI-CyD/pDNA polyplexes

The particle size and zeta potential at different N/P ratios for polyplexes are shown in Table II.

**Table II:** Physicochemical characteristics of different polyplexes

N/ P	PEI		PEI-CyD		HA-PEI-CyD1		HA-PEI-CyD2		HA-PEI-CyD3	
	Size (nm)	Zeta potential (mV)	Size (nm)	Zeta potential (mV)	Size (nm)	Zeta potential (mV)	Size (nm)	Zeta potential (mV)	Size (nm)	Zeta potential (mV)
1.25	437±23	12.1±1.7	472±19	6.2±1.1	412±19	3.4±1.9	398±17	2.27±1.8	367±12	1.3±1.1

2.5	239±17	22.9±1.3	376±16	18.3±1.7	285±16	9.2±1.4	261±11	7.93±1.2	239±9	3.4±1.5
5	201±7	36.3±1.3	281±12	33.1±1.7	271±12	24.1±1.1	252±9	16.7±1.3	237±8	13.9±1.4
7.5	193±13	35.1±1.1	268±14	29.3±1.2	259±15	19.6±1.6	237±8	15.1±1.7	219±11	12.6±1.2
10	189±16	33.7±1.4	254±13	26.1±1.9	247±18	16.1±1.2	223±11	13.6±1.5	201±9	10.8±1.4

All values are expressed as mean ± SD (n=6)

In all the polyplexes particle size was reduced upon increasing the N/P ratio from 1.25 to 10. The difference in various formulation parameters was not significant between the N/P ratios 7.5 and 10. Zeta potential was invariably increased upon increasing the N/P ratio however; zeta potential of PEI-CyD was less as compared to PEI polyplexes alone. Zeta potential was further reduced in case of HA-PEI-CyD polyplexes upon increasing the HA content from 5 to 15%. The polyplexes were found to have almost spherical shape (Figure 2 A and B).

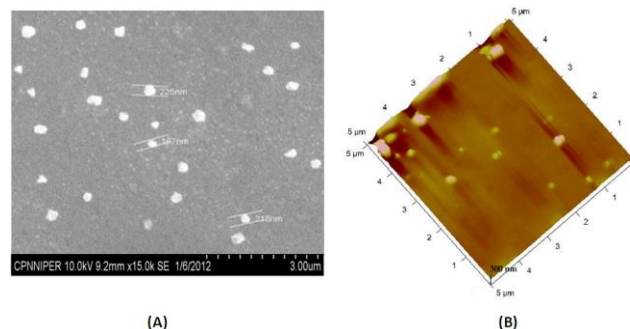


**Figure 2:** Shape and morphology of HA-PEI-CyD1 at N/P ratio 10 (A) SEM (B) AFM

### 3.3 Agarose gel electrophoresis

A complete retardation of electrophoretic mobility was observed at N/P ratio 1.25 in case of PEI polyplexes while this was shifted towards higher N/P ratios in case of CyD and HA conjugated polyplexes (Figure 3).



**Figure 3:** Agarose gel electrophoresis. Lane 1 represents uncomplexed pDNA while Lane 2-6 represents polyplexes at 1.25, 2.5, 5, 7.5 and 10 respectively

However, complete electrophoretic retardation was observed at N/P ratio 7.5 for all the complexes yet N/P ratio 10 was implemented for further studies based on our previous experience (Table II).

### 3.4 DNase protection assay

Cleavage of DNA in presence of DNase results in formation of nucleotide which is confirmed by increased absorbance at 260 nm. The change in absorbance for different polyplexes is shown in Figure 4.

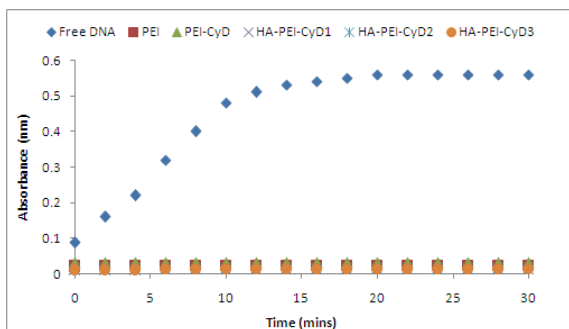


**Figure 4: DNase protection assay. Plot indicates change in absorbance with time**

Naked pDNA cleaved to nucleotide in presence of DNase, as evident by the increased absorbance up to 10 min at 260 nm. Different polyplexes were able to protect the complexed pDNA, as no change in absorbance value was observed at different time points. Although the protection efficiency of all polyplexes was significantly ( $p < 0.001$ ) higher in comparison with naked pDNA yet, difference was insignificant ( $p > 0.05$ ) among different polyplexes. The results clearly indicated that pDNA complexed with PEI was resistant to nucleases attack irrespective of the presence of CyD and HA in PEI backbone.

The electrophoretic movement of pDNA is shown in Figure 2B. No electrophoretic mobility was observed in case of naked pDNA incubated in presence of DNase while the electrophoretic mobility was retained (Figure 5, lane 3-7) in case of different polyplexes.

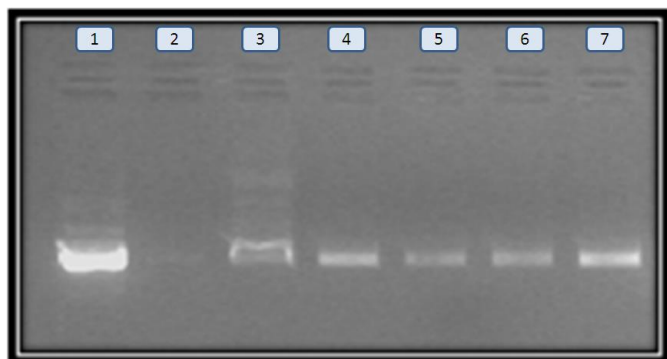


**Figure 5: DNase protection assay. Lane 1: pDNA without DNase treatment; lane 2: pDNA incubated with DNase; lane 3-4: PEI and PEI-CyD; lane 5-7: HA-PEI-CyD (1-3)**

### 3.5 Serum stability

#### 3.5.1 Physicochemical characterization

The influence of serum on particle size and zeta potential of the formulated polyplexes is shown in Table III.

**Table III: Physicochemical characteristics of different formulations after exposure to serum**

Formulation	Size (nm)		Zeta Potential (mV)	
	Before	After	Before	After
PEI	189±16	557±18	+33.7±1.4	-24.3±1.6
PEI-CyD	254±13	457±31	+26.1±1.9	+4.4±1.2
HA-PEI-CyD1	247±18	268±19	+16.1±1.2	+12.1±1.3
HA-PEI-CyD2	223±11	247±11	+13.6±1.5	+10.5±1.8
HA-PEI-CyD3	201±9	223±9	+10.8±1.4	+7.6±1.4

Values are expressed as Mean ± SD (n=6)

A drastic increase in size and reduction in zeta potential was observed in case of PEI and PEI-CyD polyplexes while all the HA-

PEI-CyD (1-3) polyplexes were found quite stable, as only a slight increase in size and decrease in zeta potential was observed.

#### 3.5.2 EtBr intercalation assay

Change in fluorescent intensity observed in case of different complexes is shown in Figure 6. Percentage change in EtBr fluorescence was significantly higher ( $p < 0.001$ ) in case of PEI and PEI-CyD indicative of lesser stability of these complexes in presence of serum while HA-PEI-CyD polyplexes were quite stable as evident by almost constant fluorescence intensity till 4 h.

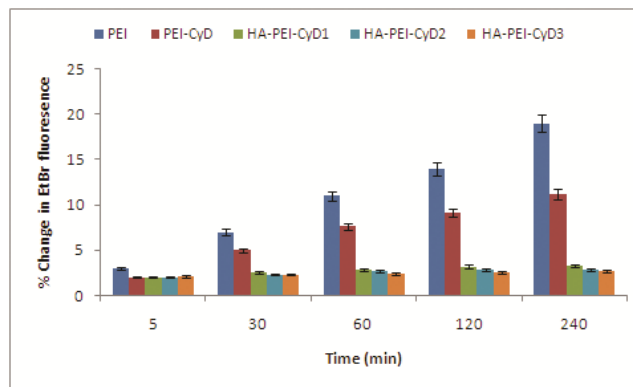


**Figure 6: Stability of different polyplexes in presence of serum. Plot indicates the % change in EtBr fluorescence with respect to time**

#### 3.6 In vitro transfection efficiency

The in vitro transfection efficiency of the developed non viral vectors was assessed as a function of qualitative and quantitative tools. Confocal images of the cells treated with various transfecting agents and developed novel vectors revealed that HA modified complexes exhibited remarkably higher fluorescence in comparison with PEI and PEI-CyD in all the cell lines. However, fluorescence observed in HeLa and HEK-293 cell lines was much higher in comparison with MCF-7 cell lines (Figure 7).

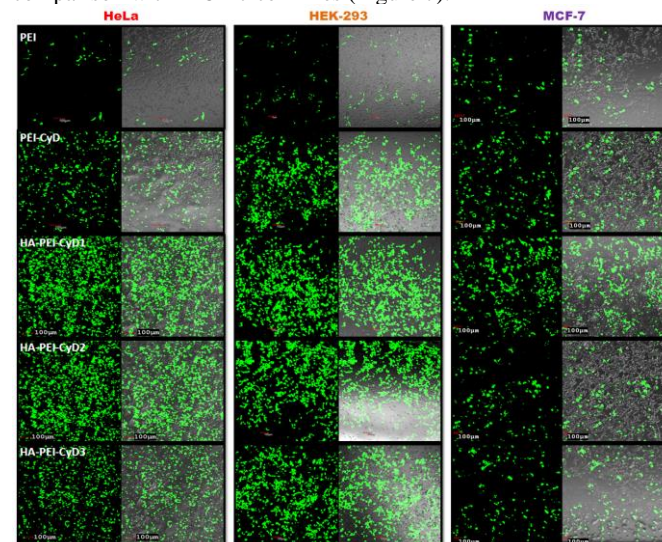


**Figure 7: CLSM images of HeLa, HEK-293 and MCF-7 cells. For each incubation type, the left and right panels represent GFP fluorescence (green) and overly of GFP and DIC (Differential interference contrast image)**

Concomitantly, similar results were also noted in case of flow cytometry assessment wherein >80% cell transfection was noted for

HA-PEI-CyD in HeLa and HEK 293 cells. In contrast, ~20% and ~40% transfection efficiency was noted in case of PEI and PEI-CyD, respectively in all the cell lines. Interestingly, in case of HA-PEI-CyD, the lower transfection efficiency (~50%) was noted in MCF-7 cell lines which was almost comparable with that of PEI-CyD (~40%) (Figure 8). The results could be attributed to the relative overexpression of CD44 receptors on HeLa and HEK 293 cell lines as compared to that of MCF-7 cells. Further, the quantitative estimation of cell transfection using fluorescence spectrophotometer suggested 4.1, 6.5 and 5.7 fold enhanced transfection in comparison with PEI alone in HeLa, HEK-293 and MCF-7, respectively upon inclusion of CyD to PEI backbone. The highest transfection was observed in case of HA-PEI-CyD1, which was 39.5, 41.5 and 8.8 fold higher as compared to PEI while 9.6, 6.3 and 1.4 fold higher as compared to PEI-CyD in HeLa, HEK-293 and MCF-7 cell lines, respectively (Figure 9).

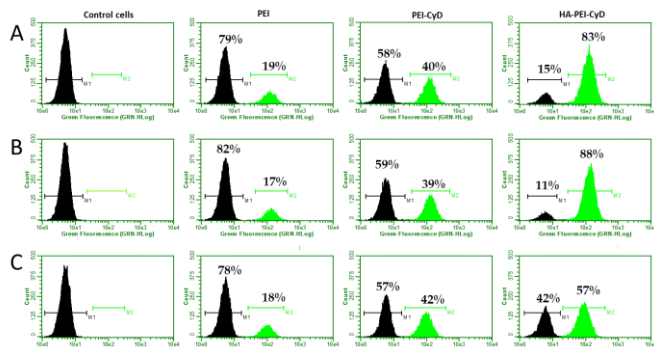


**Figure 8:** Flow cytometry based assessment of *In vitro* transfection efficiency in (A) HeLa cell lines, (B) HEK 293 cell lines and (C) MCF-7 cell lines using of PEI, PEI-CyD and HA-PEI-CyD polyplexes

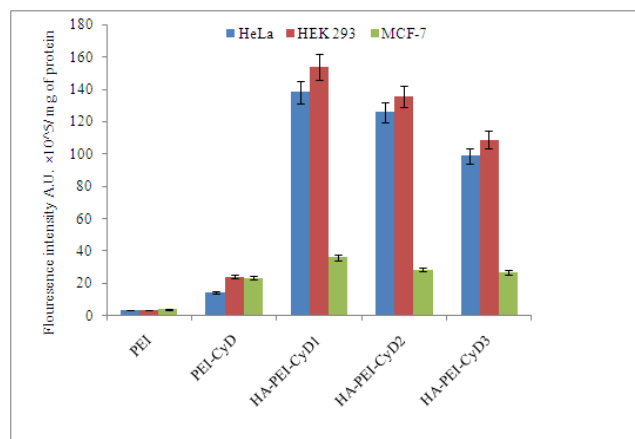


**Figure 9:** Transfection efficiency of PEI, PEI-CyD and HA-PEI-CyD polyplexes in different cell lines

### 3.7 Cytotoxicity assay

Percent cell viability in case of PEI polyplexes was found to be < 25% while it was  $\geq 70\%$  in case of PEI-CyD in all the cell lines. Further modification with HA resulted in > 90% cell viability in case of HA-PEI-CyD polyplexes which was significantly higher in comparison with PEI ( $p < 0.001$ ) and PEI-CyD ( $P < 0.05$ ). Although percentage of cell viability was slightly increased upon increasing the HA concentration yet, it was insignificant ( $p > 0.05$ ) (Figure 10).

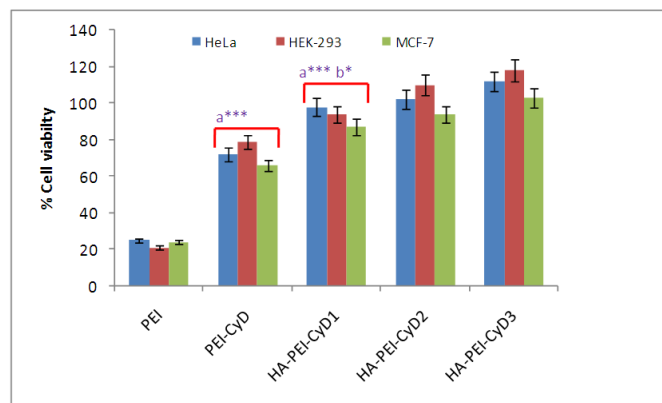


**Figure 10:** *In vitro* cell viability of HeLa, HEK-293 and MCF-7 cells incubated with various polyplexes (a; in comparison with PEI, b; in comparison with PEI-CyD) (\*\* $p < 0.001$ , \* $p < 0.05$ )

### 3.8 Cell uptake and colocalization studies

For cell uptake and colocalization, HA-PEI-CyD1 was taken into consideration as it exhibited highest transfection and compared with PEI and PEI-CyD as basic and intermediate products. Representative confocal images of HeLa, HEK-293 and MCF-7, cells incubated with different complexes are shown in Figure 11.

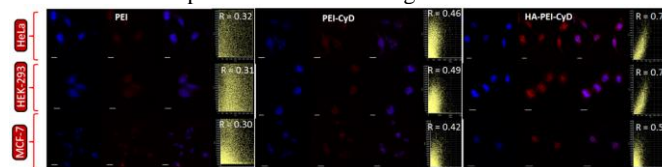


**Figure 11:** Confocal microscopic images of HeLa, HEK-293 and MCF-7 cell lines treated with RITC-complexes. The white line represents scale bar of 10 nm. The left, middle and right panel of each incubation type represents RITC fluorescence, an overlay of RITC and DAPI fluorescence and scatter plot analysis for the entire field of view. The horizontal and vertical axes of each scatter plot represents the values of pixels in channel 2 (ch2) and channel 1(ch1) respectively

As evident from the images, HA modified complex exhibited qualitatively very high internalization in all the three cell lines. Moreover, the highest colocalization coefficient was observed in case of HA modified complexes ( $r > 0.5$  in all the cell lines), followed by PEI-CyD and PEI polyplexes.

### 3.9 *In vitro* hemocompatibility

Hematological parameters were affected significantly in case of PEI while it was insignificant in case of developed polyplexes (data not shown). Hemolytic toxicity profile and % hemolysis observed in case of different complexes is shown in Figure 12 A and B, respectively.

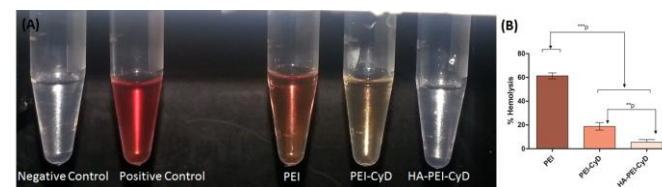


**Figure 12:** Hemocompatibility of different complexes (A) Color produced as a result of hemoglobin oxidation (B) percent hemolysis. (\*\* $p < 0.001$ , \*\* $p < 0.01$ ) ( $n = 3$ )

Complete lysis was observed in case of positive control (distilled water) and considered 100% while no hemolysis was observed in case of negative control (PBS, pH 7.4). Incubation of RBCs with

PEI led to significant hemolysis ( $P < 0.001$ ) as compared to PEI-CyD and HA-PEI-CyD. Furthermore, PEI-CyD also showed significant ( $p < 0.01$ ) hemolysis as compared to HA-PEI-CyD.

### 3.10 *In vivo* gene expression

In order to confirm the delivery potential of the designed conjugate *in vivo* gene expression study was designed in which different conjugates as well as free DNA were injected intratumorally and green fluorescence produced as a result of gene expression was observed. Intense fluorescence was observed in all the complexes while the fluorescence was negligible in case of free DNA (Figure 13).

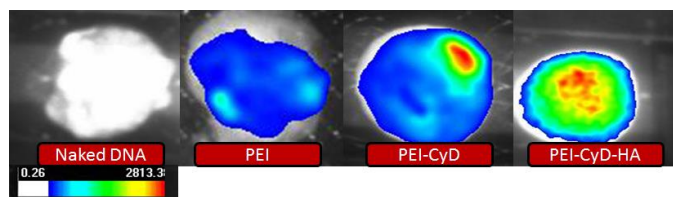


**Figure 13:** Images of the excised tumors showing GFP expression following intratumoral injection of naked plasmid DNA and different polyplexes in tumor bearing rats

### 3.11 *In vivo* toxicity

Change in different biochemical markers following the administration of different polyplexes is shown in Figure 14.

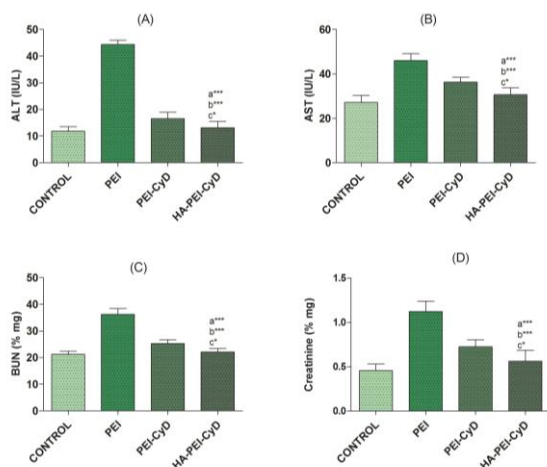


**Figure 14:** Levels of serum biochemical markers (A) ALT (B) AST (C) BUN (D) Creatinine following intravenous administration of PEI, PEI-CyD and HA-PEI-CyD polyplexes

No significant difference, in levels of various biochemical parameters viz. ALT and AST for liver function (Figure 14 A and B), and BUN and creatinine (Figure 14 C and D) for renal function was observed in case of HA-PEI-CyD while they were significantly changed ( $P < 0.001$ ) in case of PEI and PEI-CyD polyplexes in comparison with control.

## 4. Discussion

In the present work HA-PEI-CyD based polyplexes were developed with the assumption that inclusion of CyD and HA will provide dual specification and fortify the efficacy of the developed system. For the purpose, HA-PEI-CyD was synthesized and characterized by proton NMR. Following synthesis the polyplexes were formed at different N/P ratio by incubating the synthesized conjugate with DNA. The formation of polyplexes was based on the principle of

electrostatic attraction between positively charged amino groups of HA-PEI-CyD and negatively charged phosphate groups of DNA. The size and surface charge of particles play an important role in cellular uptake as positively charged complex interacts with the negatively charged proteoglycans of the cell membrane which results in enhanced cellular uptake over neutral and negatively charged complexes. In all the polyplexes particle size was reduced which could be attributed to the condensation of the negatively charged plasmid DNA with increasing amount of cationic counterpart. Among the different N/P ratios tested, minimum particle size observed at N/P ratios 7.5 and 10 might be the consequence of formation of most condensed structure due to the balance between the positive and negative charge moieties. Higher size at N/P ratios  $> 10$  could be ascribed to the formation of loosely packed aggregates due to excessive positive charge (data not shown). Conjugation of CyD to PEI resulted in larger complex while increasing concentration of HA resulted in formation of small sized complexes. The results are in agreement with our previous observation and could be attributed to the formation of more condensed and spherical structures due to strong electrostatic attraction.<sup>17</sup> Invariable increase in zeta potential upon increasing the N/P ratio could be ascribed to the obvious reason of higher concentration of cationic counterpart. Comparative lesser zeta potential of PEI-CyD and HA-PEI-CyD to PEI polyplexes might be the consequences of some degree of capping of positively charged amino groups by CyD. The results are in agreement with previous reports.<sup>29</sup>

Conjugation of PEI with CyD and HA can negatively influence the complexation efficiency of PEI to pDNA. In order to determine the effect of conjugation of PEI with CyD and HA agarose gel electrophoresis was performed at different N/P ratios (1.25, 2.5, 5, 7.5 and 10). Shifting of N/P ratio could be attributed to the some degree of capping of a fraction of positively charged amino groups of PEI by bulky CyD and HA, rendering them inaccessible for binding to DNA. This was further confirmed by shifting the N/P ratio towards higher side upon increasing the HA concentration from HA-PEI-CyD (1-3). Higher concentration of HA might have blocked more number of amino groups and therefore reduced their availability for complexation with pDNA.

DNase assay is based on the principle of degradation of free DNA in presence of DNase. An ideal gene delivery reagent is expected to provide protection against nuclease present in different biological fluids. Stability of complexed pDNA in polyplexes could be attributed to the strong electrostatic attraction between positively charged amine groups of PEI and negatively charged phosphate groups of pDNA.

In another approach, protection of pDNA complexed in different polyplexes was confirmed by gel electrophoresis. Incubation of polyplexes with heparin solution resulted in displacement of pDNA from the complex due to high binding efficiency of heparin to PEI in comparison to pDNA. This displaced free pDNA exhibited electrophoretic mobility in gel electrophoresis. No electrophoretic mobility in case of naked pDNA could be attributed to the degradation of pDNA and complete loss of electrophoretic mobility while retention of electrophoretic mobility in case of different complexes might be the consequence of protection of complexed pDNA against DNase I. The results of gel electrophoresis further supported our previous observation in which protection efficiency of complexes was evaluated by measuring the change in absorbance. Serum stability of polyplexes is important parameter which directly influences the *in vivo* performance of the polyplexes. Cationic PEI polyplexes are known to interact with anionic proteins in serum

which results in formation of larger size aggregates. This ultimately leads to reduced endocytosis and poor transfection efficiency.<sup>30</sup> Reduction of protein adsorption by several means has been shown to improve transfection efficiency.<sup>31</sup> Therefore, serum stability was taken as quality control tool to determine the stability of developed complexes in presence of serum. A drastic increase in size and reduction in zeta potential observed in case of PEI and PEI-CyD polyplexes could be attributed to the adsorption of negatively charged serum proteins over the positively charged polyplexes due to strong electrostatic attraction. This observation was in agreement with previous reports.<sup>32</sup> Improved stability of all the HA-PEI-CyD (1-3) polyplexes could be contributed by partial neutralization of excessive positive charge by HA which ultimately decreased the tendency of protein adsorption due to reduced electrostatic attraction. Along with changes in physicochemical characteristics negatively charged proteins can also displace the complexed DNA. For the purpose EtBr intercalation assay was performed which is based on the principle of intercalation of EtBr between the base pairs of double helix of displaced DNA which results in emission of intense fluorescence signal at 618 nm when excited at 516 nm. High charge density over the PEI and PEI-CyD could provide strong electrostatic attraction with serum proteins which might have led to displacement of pDNA from the complex and destabilization of these complexes. Surface modification of PEI using different concentrations of HA resulted in masking of excessive positive charge which could stabilize the system in presence of serum by reducing excessive adsorption of serum proteins.

The transfection efficiency of a gene delivery reagent is not only dependent upon the purity of gene construct but also equally contributed by the efficacy and target specificity of the delivery vehicle. Further, specialized uptake mechanisms and over expression of specific receptors on different cells necessitates the design of surface engineered delivery reagents which can deliver the gene construct more specifically to target cells. To provide target specificity, HA was appended on PEI-CyD backbone which binds specifically to CD44 receptors. These receptors have been reported to over express on a variety of tumor cells viz. breast, colon, bowel, brain, melanoma, sarcoma, renal and prostate.<sup>17</sup> To exactly mimic and evaluate the effect of over expression, HeLa, HEK-293 and MCF-7 cell lines were used to estimate *in vitro* transfection efficiency. Selection of cell lines was based on level of expression of CD44 receptors; as CD44 shows over expression in HeLa and HEK-293<sup>17, 18</sup> while low level of expression in MCF-7.<sup>33</sup> Higher fluorescence observed in case of HA modified PEI-CyD could be attributed to the enhanced uptake of the polyplexes through receptor mediated endocytosis. Furthermore, quite higher fluorescence in case of HeLa and HEK-293 in comparison with MCF-7 might be the consequences of over-expression of HA receptors in HeLa and HEK-293 cell lines while low level of expression in MCF-7. In line with previous reports inclusion of CyD to PEI backbone could fortify the transfection efficiency.<sup>29</sup> CyDs are cup-shaped cyclic oligomers of glucose which have been well recognized for their importance in gene transfection. By forming inclusion complexes via host-guest interaction, CyDs provide facile and versatile attachment sites for ligands anchorage.<sup>29</sup> Based on the outcomes of our previous work we speculated that inclusion of CyD can improve the efficacy of targeted transfection by providing multiple attachment sites to HA. As both HA and pDNA are negatively charged they can compete with each other for binding to PEI and can adversely affect the performance. Therefore, attachment of HA as inclusion complex, can prevent such unnecessary competition. In line, HA modification could result into improved transfection while diminished transfection observed at higher concentration of HA (HA-PEI-CyD2 and HA-

PEI-CyD3) could be attributed to the masking of additional charge of PEI by excess HA while at low concentration (5%) almost whole HA could be utilized to form inclusion complexes without much affecting the positively charged amino groups of PEI. In support of our hypothesis HA-PEI-CyD exhibited significantly higher transfection efficiency in comparison with our previously reported HA-PEI polyplexes.<sup>17</sup>

Although, PEI based complexes have been recognized for their tremendous potential in gene delivery yet, fraught with major limitation of higher cell cytotoxicity due to excessive positive charge density of these systems. Excessive positive charge and molecular weight are two major factors which have been recognized to exhibit high cytotoxicity.<sup>17, 18</sup> In order to nullify the excessive charge, PEI was first modified with CyD to obtain PEI-CyD that was further modified by anchoring targeting ligand HA to PEI-CyD backbone. Significantly higher cell viability observed in case of HA-PEI-CyD could be attributed to the capping of additional charge of PEI by CyD and HA. Lower toxicity at higher concentration of HA could be ascribed to the same reason of neutralization of charge on PEI.

In order to understand the underlying mechanism behind the much higher transfection in HA modified complexes comparative cell uptake and colocalization studies were performed using CLSM and flow cytometry. Significantly higher internalization could be attributed to the receptor mediated uptake due to HA modification which facilitated their binding and internalization through interaction with CD44 receptors on cell membranes.<sup>17</sup> By this observation we speculated that this higher transfection may be the result of efficient nuclear colocalization of the HA modified complex. Thus our next step was to elucidate the delivery efficiency of the HA modified complex to deliver the loaded DNA into the site of transfection i.e. nucleus. A colocalization coefficient greater than or equal to 0.5 ( $r \geq 0.5$ ) is usually considered as an indicator of efficient colocalization.<sup>34</sup> A good colocalization coefficient observed in our case can be rationalized by concentrating on the stability profile of individual formulation in presence of serum. As evident from Table 3, PEI-polyplexes displayed negative charges in presence of serum while it was reduced noticeably in case of PEI-CyD polyplexes. HA modified complexes were quite stable as no significant change in size and charge was observed. Thus, amongst all the investigated complexes, only HA modified complexes are supposed to retain sufficient positive charges in the intracellular milieu to get internalized and rapid endolysosomal escape via proton sponge effect and subsequent colocalization in the nucleus.

In line with our concept synthesized conjugate demonstrated better compatibility in comparison to PEI and PEI-CyD polyplexes and could be directly related to capping of excess cationic groups of PEI. Further in order to confirm the delivery potential of the designed conjugate *in vivo* gene expression study was designed in which different conjugates as well as free DNA were injected intratumorally and green fluorescence produced as a result of gene expression was observed. In line with our hypothesis the HA-PEI-CyD expressed much higher fluorescence in comparison with PEI and PEI-CyD complexes. The enhanced efficacy observed in case of HA-PEI-CyD could be correlated with our *in vitro* results in which HA modification resulted in improved stability in comparison to other complexes. Furthermore, receptor mediated uptake due to HA modification and rapid endolysosomal escape via proton sponge effect and subsequent colocalization in the nucleus could improve the overall performance.

In order to further prove the improved safety profile of the developed polyplexes *in vivo* toxicity studies were performed. These *in vivo* findings are quite consistent with our previous observations

of cytotoxicity assay on different cell lines and further strengthen the concept that masking of excessive charge of PEI can be utilized as a fruitful strategy to overcome toxicity related issues. Simultaneously, careful selection of the compounds in system fabrication can be used to control the intracellular trafficking as desirable.

### 5. Conclusions

The proposed HA-PEI-CyD was found to have better transfection efficiency and lower cytotoxicity in comparison with PEI-CyD and previously reported HA-PEI in different cell lines which strongly support the suitability of the system in designing delivery reagent with target specificity. The system further provides an insight to develop a variety of gene delivery construct by considering different targeting ligands. Encouraged with findings we are at the stage of evaluating in vivo bio-distribution and gene expression following intravenous administration which will be reported over time.

### Acknowledgement

Authors are thankful to Indian National Science Academy (INSA), Government of India, New Delhi, for providing financial assistance, Council of Scientific and Industrial Research (CSIR) Govt. of India, India for providing fellowship to Mr. AKA and KT and Director, NIPER for providing necessary infrastructure facilities.

### References

<sup>a</sup>Centre for Pharmaceutical Nanotechnology, Department of Pharmaceutics,

<sup>b</sup>Department of Pharmaceutical Technology,

National Institute of Pharmaceutical Education and Research (NIPER), Sector 67, S.A.S. Nagar (Mohali) Punjab- 160062 INDIA, Telephone: 0172-2292055, Fax: 0172-2214692, E-mail: sanyogjain@niper.ac.in; sanyogjain@rediffmail.com

† Electronic Supplementary Information (ESI) available. See DOI: 10.1039/b000000x/

1. S. C. De Smedt, J. Demeester and W. E. Hennink, *Pharm. Res.*, 2000, **17**, 113-126.
2. S. A. Audouy, L. F. de Leij, D. Hoekstra and G. Molema, *Pharm. Res.*, 2002, **19**, 1599-1605.
3. D. J. Glover, H. J. Lipps and D. A. Jans, *Nat. Rev. Genet.*, 2005, **6**, 299-310.
4. G. D. Schmidt-Wolf and I. G. Schmidt-Wolf, *Trends Mol. Med.*, 2003, **9**, 67-72.
5. T. Bronich, *Pharm. Res.*, 2010, **27**, 2257-2259.
6. B. H. Zinselmeyer, S. P. Mackay, A. G. Schatzlein and I. F. Uchegbu, *Pharm. Res.*, 2002, **19**, 960-967.
7. D. W. Pack, A. S. Hoffman, S. Pun and P. S. Stayton, *Nat. Rev. Drug Discov.*, 2005, **4**, 581-593.
8. V. Vijayanathan, T. Thomas and T. J. Thomas, *Biochemistry*, 2002, **41**, 14085-14094.
9. H. Aldawsari, B. S. Raj, R. Edrada-Ebel, D. R. Blatchford, R. J. Tate, L. Tetley and C. Dufes, *Nanomed.*, 2011, **7**, 615-623.
10. D. Jiang and A. K. Salem, *Int. J. Pharm.*, 2012, **427**, 71-79.
11. C. H. Ahn, S. Y. Chae, Y. H. Bae and S. W. Kim, *J. Control. Release*, 2002, **80**, 273-282.
12. B. Liang, M. L. He, C. Chan, Y. Chen, X. P. Li, Y. Li, D. Zheng, M. C. Lin, H. F. Kung and X. T. Shuai, *Biomaterials*, 2009, **30**, 4014-4020.
13. S. Kommareddy and M. Amiji, *Nanomed.*, 2007, **3**, 32-42.
14. G. P. Tang, J. M. Zeng, S. J. Gao, Y. X. Ma, L. Shi, Y. Li, H. P. Too and S. Wang, *Biomaterials*, 2003, **24**, 2351-2362.
15. S. Kawakami, A. Sato, M. Nishikawa, F. Yamashita and M. Hashida, *Gene Ther.*, 2000, **7**, 292-299.
16. S. Patnaik, A. Aggarwal, S. Nimesh, A. Goel, M. Ganguli, N. Saini, Y. Singh and K. Gupta, *J. Control. Release*, 2006, **114**, 398-409.

17. A. Pathak, A. Swami, S. Patnaik, S. Jain, K. Chuttani, A. K. Mishra, S. P. Vyas, P. Kumar and K. C. Gupta, *J. Biomed. Nanotechnol.*, 2009, **5**, 264-277.
18. A. Pathak, P. Kumar, K. Chuttani, S. Jain, A. K. Mishra, S. P. Vyas and K. C. Gupta, *ACS Nano*, 2009, **3**, 1493-1505.
19. H. Yao, S. S. Ng, W. O. Tucker, Y. K. T. Tsang, K. Man, X. Wang, B. K. C. Chow, H. F. Kung, G. P. Tang and M. C. Lin, *Biomaterials*, 2009, **30**, 5793-5803.
20. S. H. Pun, N. C. Bellocq, A. Liu, G. Jensen, T. Macheimer, E. Quijano, T. Schlup, S. Wen, H. Engler, J. Heidel and M. E. Davis, *Bioconjug. Chem.*, 2004, **15**, 831-840.
21. X. Q. Zhang, X. L. Wang, P. C. Zhang, Z. L. Liu, R. X. Zhuo, H. Q. Mao and K. W. Leong, *J. Control. Release*, 2005, **102**, 749-763.
22. S. Jain, S. Kumar, A. K. Agrawal, K. Thanki and U. C. Banerjee, *Mol. Pharmaceutics*, 2013, **10**, 2416-2425.
23. S. Jain, S. R. Patil, N. K. Swarnakar and A. K. Agrawal, *Mol. Pharmaceutics*, 2012, **9**, 2626-2635.
24. A. K. Agrawal, H. Harde, K. Thanki and S. Jain, *Biomacromolecules*, 2014, **15**, 350-360.
25. S. Hwa Kim, J. Hoon Jeong, C. O. Joe and T. Gwan Park, *J. Control. Release*, 2005, **103**, 625-634.
26. S. Li, W. C. Tseng, D. B. Stolz, S. P. Wu, S. C. Watkins and L. Huang, *Gene Ther.*, 1999, **6**, 585-594.
27. S. P. Kasturi, K. Sachaphibulkij and K. Roy, *Biomaterials*, 2005, **26**, 6375-6385.
28. S. Jain, P. U. Valvi, N. K. Swarnakar and K. Thanki, *Mol. Pharmaceutics*, 2012, **9**, 2542-2553.
29. M. L. Forrest, N. Gabrielson and D. W. Pack, *Biotechnol. Bioeng.*, 2005, **89**, 416-423.
30. M. Bello Roufai and P. Midoux, *Bioconjug. Chem.*, 2001, **12**, 92-99.
31. P. R. Dash, M. L. Read, K. D. Fisher, K. A. Howard, M. Wolfert, D. Oupicky, V. Subr, J. Strohalm, K. Ulbrich and L. W. Seymour, *J. Biol. Chem.*, 2000, **275**, 3793-3802.
32. S. Li, M. A. Rizzo, S. Bhattacharya and L. Huang, *Gene Ther.*, 1998, **5**, 930-937.
33. X. Sun, P. Ma, X. Cao, L. Ning, Y. Tian and C. Ren, *Drug Deliv.*, 2009, **16**, 357-362.
34. S. R. Dattir, M. Das, R. P. Singh and S. Jain, *Bioconjug. Chem.*, 2012, **23**, 2201-2213.